Hydrogeology Journal (2014) 22: 251–262
DOI 10.1007/s10040-013-1052-6

Effects of regional groundwater flow on the performance of an aquifer thermal energy storage system under continuous operation

Kun Sang Lee

Abstract Numerical investigations and a thermohydraulic evaluation are presented for two-well models of an aquifer thermal energy storage (ATES) system operating under a continuous flow regime. A three-dimensional numerical model for groundwater flow and heat transport is used to analyze the thermal energy storage in the aquifer. This study emphasizes the influence of regional groundwater flow on the heat transfer and storage of the system under various operation scenarios. For different parameters of the system, performances were compared in terms of the temperature of recovered water and the temperature field in the aquifer. The calculated temperature at the producing well varies within a certain range throughout the year, reflecting the seasonal (quarterly) temperature variation of the injected water. The pressure gradient across the system, which determines the direction and velocity of regional groundwater flow, has a substantial influence on the convective heat transport and performance of aquifer thermal storage. Injection/production rate and geometrical size of the aquifer used in the model also impact the predicted temperature distribution at each stage and the recovery water temperature. The hydrogeological-thermal simulation is shown to play an integral part in the prediction of performance of processes as complicated as those in ATES systems.

Keywords Thermal conditions · Aquifer thermal energy storage · Numerical modeling · Groundwater flow · Continuous operation

Received: 20 December 2012 / Accepted: 11 September 2013
Published online: 2 October 2013

Published in the theme issue "Hydrogeology of Shallow Thermal Systems"

K. S. Lee (✉)
Department of Natural Resources and Environmental Engineering, Hanyang University, Seoul, 133-791, South Korea
e-mail: kunslee@hanyang.ac.kr
Tel.: +82-2-22202240

Introduction

As fossil fuel resources such as oil, natural gas, and coal are increasingly less available and more expensive, many energy conservation strategies become more feasible. Thermal energy storage-system applications around the world have been known to provide economical and environmentally sound solutions to the problems of energy supply (Paksoy et al. 2004). Though thermal energy storage systems themselves do not produce energy, energy storage applications for energy conservation lead to the introduction of more efficient, integrated energy systems. Thermal energy storage, therefore, makes it possible to more effectively utilize renewable energy sources (solar, geothermal, or ambient) and waste heat/cold recovery for space heating and cooling.

The storage medium may be located in containers of various types and sizes. Underground thermal energy storage is one form that is well suited to long-term and even seasonal thermal energy storage and mostly used for seasonal heat/cold storage. One of more common storage types among underground thermal energy storage systems is the aquifer thermal energy storage (ATES) system, utilizing the low-temperature geothermal resource in the aquifer (Sanner 2001; Rafferty 2003). ATES, which is similar to direct-use groundwater geothermal systems, involves storage and provides for both heating and cooling on a seasonal basis. Aquifers offer a potential and economical way of storing thermal energy for long periods of time. Molz et al. (1978, 1979, 1981) described early field experiments in ATES performed to determine the feasibility of confined aquifers as temporary storage reservoirs for thermal energy. ATES systems hold great promise for energy storage and have been used successfully around the world for the seasonal storage of heat and cold energy for the purpose of heating and cooling buildings (Probert et al. 1994; Paksoy et al. 2000; Allen et al. 2000; Schmidt et al. 2003).

In carrying out ATES development projects, a numerical model based on coupled mass and energy transport theory has to be conducted on the behavior of a local subsurface geothermal system to evaluate and optimize a project design. A number of researchers have highlighted the important role of numerical modeling in the analysis of ATES systems. Papadopulos and Larson (1978) and Tsang et al. (1981) presented the computer simulation of

two cycles of a seasonal ATES experiment and comparison with field data. Molson et al. (1992) used a three-dimensional (3D) finite element model to simulate groundwater flow and energy transport in an unconfined aquifer. Probert et al. (1994) presented the thermodynamic evaluations of ATES projects and listed key aquifer properties and design parameters. Based on an elementary ATES model, Rosen (1999) performed second-law analysis to thermal-energy storage systems to assess overall system performance. Chavalier and Banton (1999) applied the random walk method of resolution to the study of energy transfer phenomena in ATES using a single injection well. Tenma et al. (2003), Lee and Jeong (2008), and Kim et al. (2010) carried out more realistic two-well model studies to examine the design of underground thermal energy storage systems. To provide basic data for design, the studies evaluated the sensitivity of parameters affecting the long-time performance of ATES. Their studies, however, derived conclusions based on the simulation results for ATES systems without considering the effects of regional groundwater flow. It has been known that the groundwater flow induced from the pressure gradient would have a significant impact on the convective heat transfer (Nagano et al. 2002; Fan et al. 2007). However, the influence of groundwater flow on the performance of ATES has not been extensively examined. To overcome a limited applicability of previous research, more comprehensive study should be established for the evaluation of the ATES systems. The present work extends previously reported research on ATES systems under groundwater flow. The main design considerations involve heat exchanges, injection/production rates and configuration of the well-aquifer system.

Coupled hydrogeological thermal simulations were undertaken in order to predict thermal behavior of aquifer and recovery temperatures from the aquifer. Analyses for a two-well system in a confined aquifer were performed in order to determine how groundwater flow in response to hydraulic gradient affects results of aquifer thermal energy storage simulations. The aim of the evaluation is to determine whether groundwater flow needs to be taken into consideration to make reliable predictions about future recovery temperatures and temperature distributions in the aquifer given the planned injection/production temperatures and rates.

Mathematical theory

To calculate temperatures of the aquifer at different locations, theoretical principles of water flow and heat transfer phenomena are explained. Among the most advanced simulators, a general simulator named UTCHEM has proved to be particularly useful for modeling multiphase transport processes under nonisothermal conditions (Center for Petroleum and Geosystems Engineering 2000). UTCHEM has been extensively verified by comparison with analytical solutions and experimental measurements for its ability to predict the flow of fluids through an aquifer.

The continuity of mass for water in association with Darcy's law is expressed as

$$\frac{\partial}{\partial t}(n\rho_{\mathrm{w}}) + \nabla\cdot(\rho_{\mathrm{w}}\mathbf{u}) = R_{\mathrm{w}} \tag{1}$$

where

n	Porosity [dimensionless]
ρ_{w}	Density of water [M L^{-3}]
$\mathbf{u}$	Darcy flux [L t^{-1}]
t	Time [t]
R_{w}	Source term [M L^{-3} t^{-1}]

The water flux from Darcy's law is

$$\mathbf{u} = -\frac{\mathbf{k}}{\mu_{\mathrm{w}}}(\nabla p - \gamma_{\mathrm{w}}\nabla z) \tag{2}$$

where $\mathbf{k}$ is the permeability tensor; μ_{w} the dynamic viscosity [M L^{-1} t^{-1}]; p the pressure [M L^{-1} t^{-2}]; z the vertical depth [L], and γ_{w} the specific gravity ($=\rho_{\mathrm{w}}g$) [M L^{-2} t^{-2}].

The energy balance equation is derived by assuming that energy is a function of temperature only and energy flux in the aquifer occurs by convection and conduction only. The resulting general heat balance equation describing nonisothermal groundwater flow in a saturated porous medium can be formulated as follows:

$$\frac{\partial T}{\partial t}[(1-n)\rho_{\mathrm{r}}C_{\mathrm{vr}} + n\rho_{\mathrm{w}}C_{\mathrm{vw}}] + \nabla\cdot(\rho_{\mathrm{w}}C_{\mathrm{vw}}\mathbf{u}T - \lambda_{\mathrm{T}}\nabla T) = q_{\mathrm{H}} - Q_{\mathrm{L}} \tag{3}$$

where

T	Aquifer temperature [T]
C_{vr}, C_{vw}	Rock and water heat capacity at constant volume [M L^{-1} t^{-2} T^{-1}]
λ_{T}	Thermal conductivity of aquifer [ML t^{-3} T^{-1}]
q_{H}	Enthalpy source per unit bulk volume [M L^{-2} t^{-2}]
Q_{L}	Heat exchange with overburden and underburden formations [M L^{-2} t^{-2}]

The heat transfer with over and underlying low-permeability layers, is assumed to be due solely to thermal diffusion and the heat equation is simplified to

$$Q_{\mathrm{L}} = \nabla\cdot(\lambda_{Te}\nabla T) \tag{4}$$

where λ_{Te} is the thermal conductivity of overburden or underburden rock [ML t^{-3} T^{-1}].

Physical effects considered in the mathematical formulation and numerical simulation can be summarized as

 DOI 10.1007/s10040-013-1052-6

follows; (1) heat convection and conduction in the aquifer, (2) heat conduction from/to confining overburden or underburden layers, (3) permeability anisotropy, (4) effective thermal conductivity, (5) regional groundwater flow, (6) gravitational effects. However, thermal dependence of density, viscosity, thermal conductivity, and heat capacity is not taken into consideration because these parameters vary little in the considered temperature range (Doughty et al. 1982). The heat transfer Eq. (3), which results from the principle of energy conservation, is coupled with the flow equation from Darcy's law (Eq. 2) and the continuity Eq. (1).

Numerical modeling

An understanding of the thermohydraulic processes in the aquifer is necessary for a proper design of an ATES system under given thermohydraulic conditions. Simulations of 3D Darcy's flow in the aquifer were carried out with a finite-difference model for groundwater flow and heat transport. The numerical model includes the effects of hydraulic anisotropy, forced and natural convections and conduction, and heat exchange with the adjacent confining strata. In order to decide the sustainability of the aquifer for energy storage application, temperatures of producing water is estimated over a 10-year period. To reduce the numerical dispersion associated with the solution of Eq. (1) in finite-difference form, a total-variation-diminishing (TVD) third-order method was used in applying the block-centered finite-difference approximation of the spatial derivative (Liu et al. 1994).

In order to estimate the parameters of an underground system, a hypothetical 3D ATES model using the open system of two wells is considered. As shown in Fig. 1, the ATES system consists of injection and production wells situated at the centers of left and right squares consisting of a 2×1 rectangular field, respectively. Water is pumped into the injection well at a constant flow rate Q at a temperature T_{inj}, and the same flow rate of water is recovered from the neighboring production well. In a large reservoir with repeated patterns, the flow is symmetric around each pair of injection–injection wells confined to the pattern. Constant pressure is specified to left and right boundaries to induce regional groundwater flow that occurs in response to hydraulic gradient, and the other boundaries are closed to flow. All the outer boundaries are represented as adiabatic, to simulate symmetry in an array. The heat transfer in the ATES was inherently coupled with heat conduction and advection by the flow of injected water and regional groundwater.

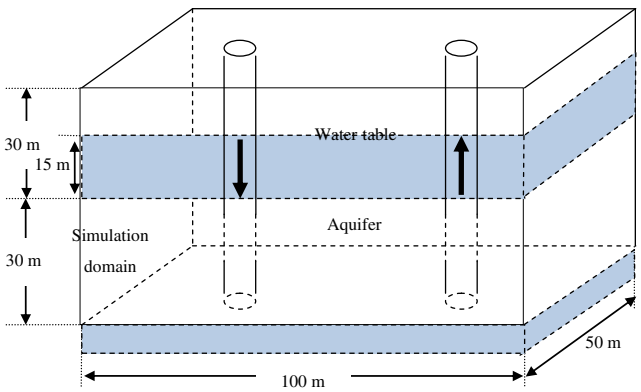

Fig. 1 Schematic representation of simulation of the base case domain

The geometry of the model is similar to that of the two-well model suggested by Tenma et al. (2003). This model is a unit of the system and is composed of two wells partially penetrating a confined aquifer. Well depth was set to be relatively shallow for the two-well system. Water level in the model was set at −15 m. Top and bottom levels of the confined aquifer were set at −30 and −60 m, respectively. Both injection and production wells were screened over the interval between −39 and −51 m. The system contacts with impervious overburden and underburden rocks which are homogeneous and have bulk thermal conductivity λ_{Te}.

The grid is divided into 26 and 13 grid blocks with maximum cell size of 5 × 5 m in x and y directions, respectively, and 10 grid blocks with uniform height in a vertical direction. Smaller grid size was used for the near-well regions where the most significant hydraulic and thermal gradients are expected.

Determination of the potential of a specific confined aquifer as an effective thermal energy storage medium requires thorough knowledge of thermodynamic and hydraulic properties of the aquifer and its confining layers and fluid properties. Parameters include porosity and permeability of the storage aquifer and thermal conductivities and heat capacities of the aquifer matrix, native groundwater, and confining layers. As presented in Table 1, the aquifer and water have constant thermal properties and are assumed to be slightly compressible. Anisotropy ratio of vertical to horizontal permeability was set to be 0.1. The aquifer is also assumed to be continuous and its thermal conductivity and volumetric heat capacity are considered to be a function of porosity and the thermal

Table 1 Hydrogeological and thermal properties of the aquifer and water

Aquifer	Porosity (n)	0.40
	Permeability (k)	1013 millidarcies (mD)
	Compressibility of formation (β_r)	2.96×10^{-6} kPa^{-1}
	Density of rock (ρ_r)	2.65 g/cm^3
	Thermal conductivity of rock (λ_T)	200 kJ/day · m · K
	Thermal conductivity of overburden/underburden rock (λ_{Te})	249.2 kJ/day · m · K
	Heat capacity of rock (C_{vr})	0.8864 kJ/kg · K
Water	Viscosity (μ_w)	1.1404 centipoise (cP)
	Compressibility (β_w)	4.4×10^{-7} kPa^{-1}
	Density (ρ_w)	1 g/cm^3
	Heat capacity (C_{vw})	4.184 kJ/kg · K

DOI 10.1007/s10040-013-1052-6

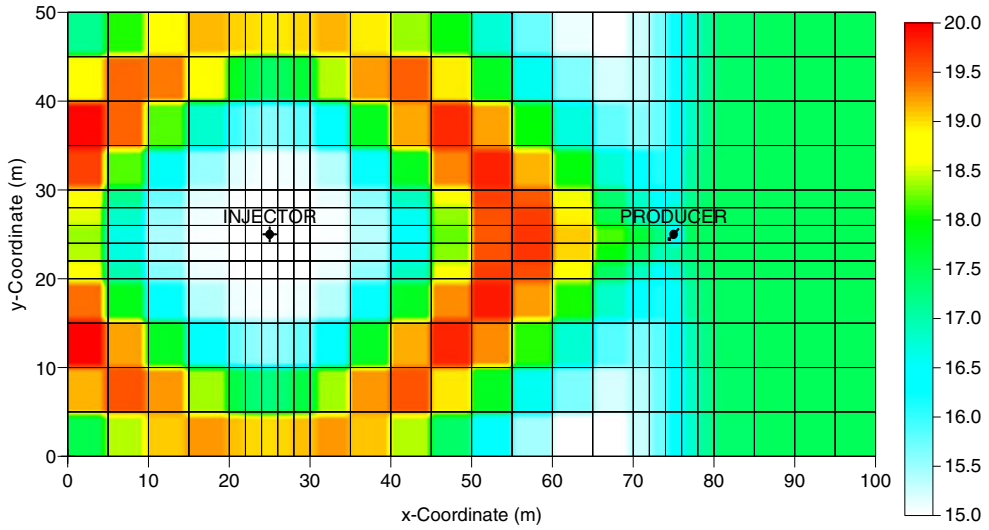

(a)

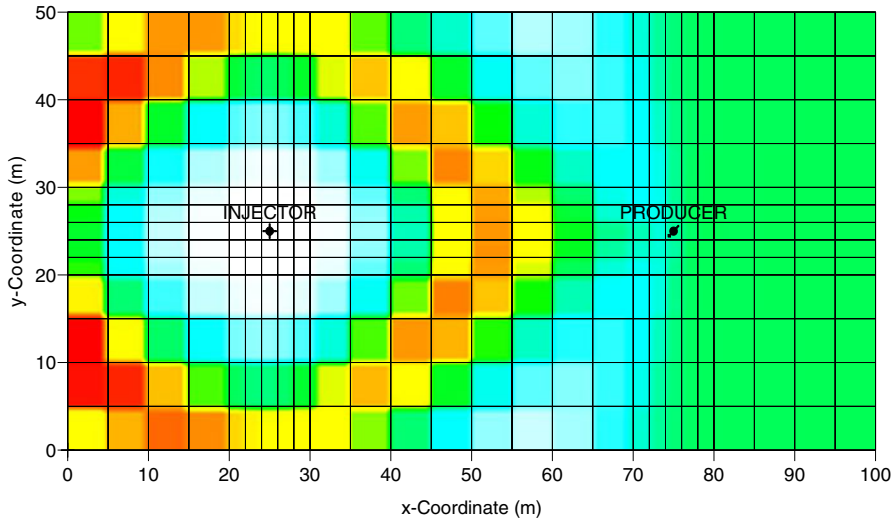

(b)

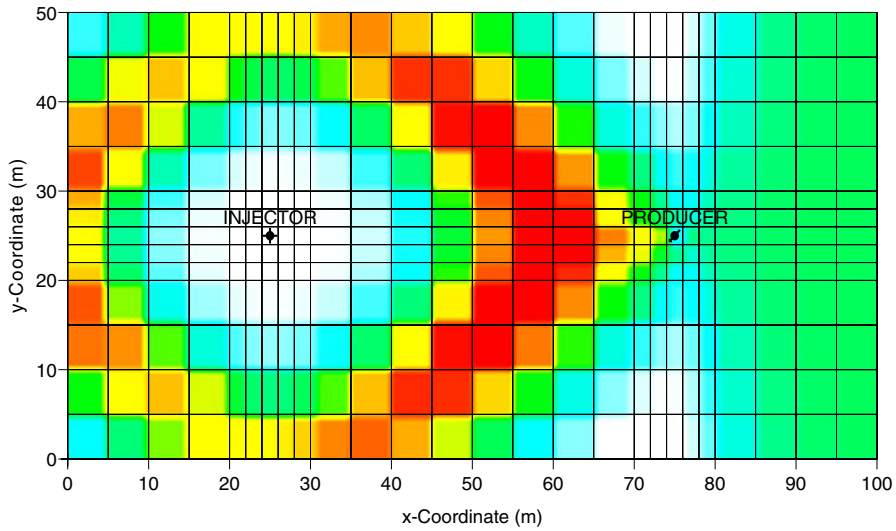

(c)

 DOI 10.1007/s10040-013-1052-6

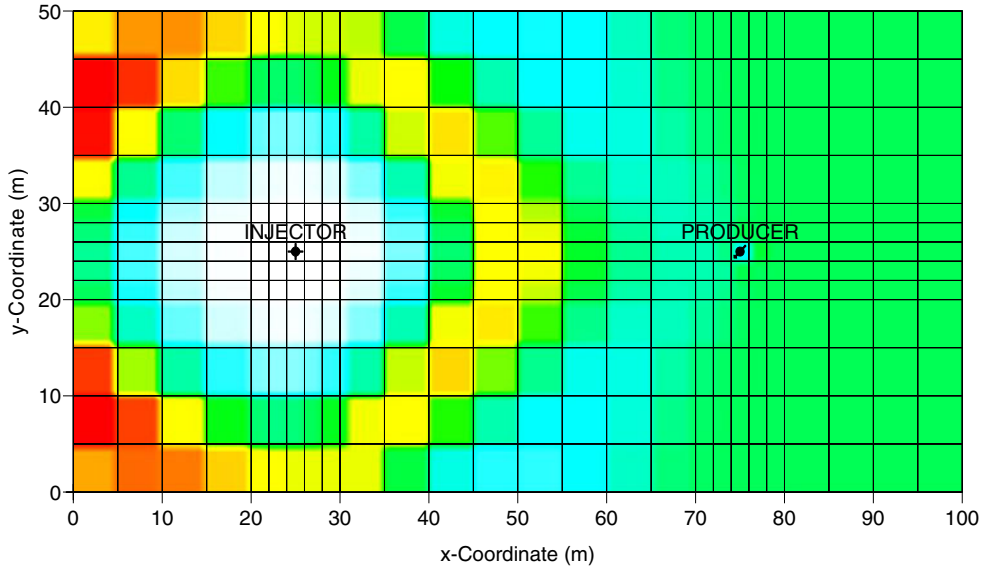

(d)

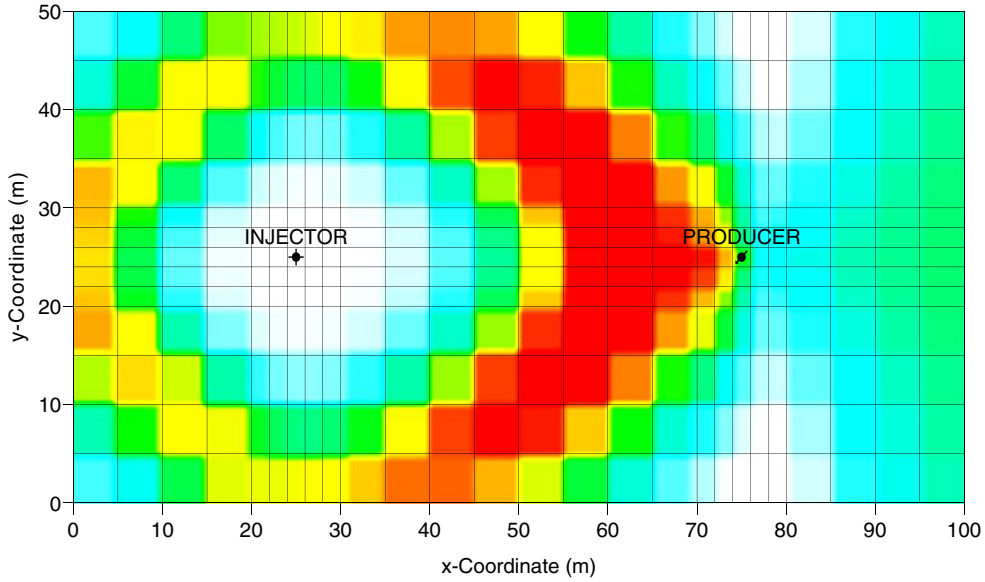

(e)

Fig. 2 (continued)

characteristics of water and soil matrix (Nassar et al. 2006).

Results and discussion

To estimate the characteristics of the system, the two-well model was run for a continuous flow regime. Heat transfer within the aquifer is simulated by specifying step-wise constant temperature T_{inj} at the injection well and with the aquifer temperature initialized at T_i. The initial temperature of the aquifer is assumed to be a constant 17.5 °C over the entire aquifer and confining layers. In the confining layers, the temperature is kept at T_i throughout the cycle and included as boundary conditions to minimize computational efforts. According to results from preliminary simulations, the difference in the amount of conductive heat exchange caused by temperature variation in the surrounding rock is very limited due to relatively small temperature difference between the aquifer and confining layers in the simulation of the ATES considered in this study. The initial pressure of the aquifer is set to be 343 kPa at −50 m. Regional groundwater flow was manifested by assigning fixed pressure conditions at specific points of left and right boundaries and included

◀ **Fig. 2** Temperature distribution [°C] obtained with different groundwater flow situations after cold water injection: **a** no groundwater flow, **b** groundwater flow from right to left (Δp = −20 kPa), **c** groundwater flow from left to right (Δp = 20 kPa), **d** groundwater flow from right to left (Δp = −40 kPa), and **e** groundwater flow from left to right (Δp = 40 kPa)

 DOI 10.1007/s10040-013-1052-6

gravity effects. The pressure difference between left (p_L) and right (p_R) boundaries at the top of the system, $\Delta p = p_L - p_R$, ranges from −40 to 40 kPa, which corresponds to the pressure gradient from −0.4 to 0.4 kPa/m. The pressure gradient in the horizontal direction derives regional groundwater flow from left to right (consistent with flow direction of injected water to the producer well) for $\Delta p > 0$ or right to left for $\Delta p < 0$. The model was run for 10 years to provide an adequate long-term assessment of thermal storage.

The ATES system was operated under a continuous flow regime, where water is pumped from one well equipped with a pump and injected through a second well. A complete energy storage cycle is composed of four periods per year to simulate the seasonal conditions. Each cycle is symmetrical for identical injection ($Q > 0$) and production ($Q < 0$) rates and duration. The thermal field and the temperature of produced water, T_{prod}, were calculated from the numerical solutions of Eq. (3) at constant time interval. Simulation results from the ATES models were compared to examine the effects of groundwater flow and various aquifer and operational parameters on the thermal plume extent and energy recovery.

Groundwater flow

Accounting for the seasonal changes in surface temperature, the injected water temperatures were taken as 5, 15, 25, and 15 °C over a 3-month period, respectively. The size of this two-well model is 100 m×50 m×30 m for the base case. The

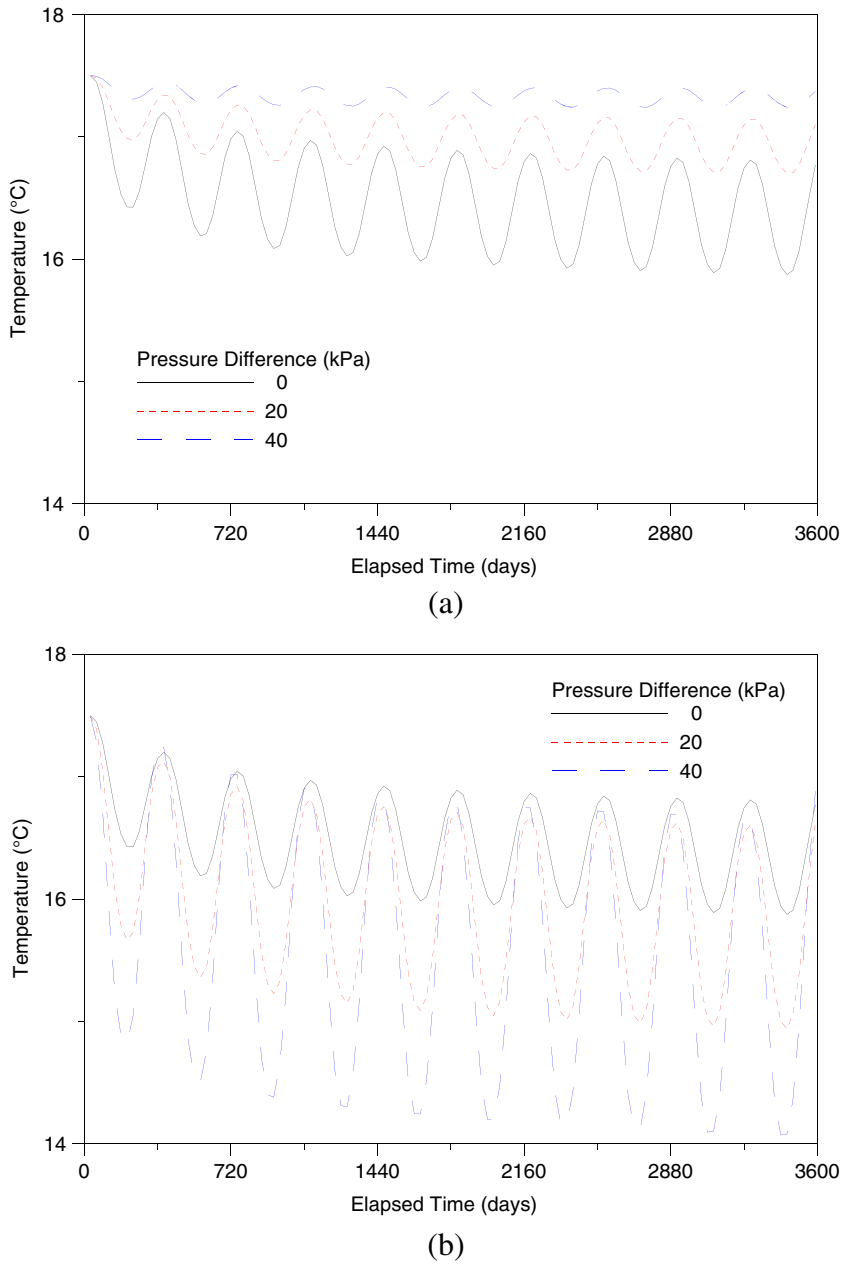

Fig. 3 Temperature of produced water obtained from simulations with different groundwater flow conditions. Groundwater flow **a** from right to left, **b** from left to right

 DOI 10.1007/s10040-013-1052-6

rates of injection or production of 100 m^3/day correspond to 0.2688 pore volume of the aquifer for 3 months.

Figure 2a–e shows temperature distribution from the numerical calculations under the boundary conditions of Δp=0 (no regional groundwater flow), −20, −40 (regional groundwater flow from right to left), 20, and 40 kPa (regional groundwater flow from right to left) at 3,600 days after 90 days of cold water injection. From the figures, the effect of groundwater flow is evident from the observation that thermal plume increasingly spreads to the production well for Δp<0. When the direction of regional groundwater flow is the same with that of injected water, the thermal front approaches the producing well much closer due to increased thermal convection.

Simulation studies on the heat transfer in the ATES system have been carried out with and without the presence of regional groundwater flow. The temperatures of produced water are shown in Fig. 3. A small variation is the most desirable case, representing sustainable use of the aquifer as a thermal energy storage system. As shown in Fig. 3, the temperature gradually decreases in all the cases. As the temperature of the circulated fluid changes in the range of 5–25 °C, the temperature eventually becomes 15 °C, the average temperature of injected water. Due to energy imbalance between the initial temperature of 17.5 °C and average injecting temperature of 15 °C, the aquifer undergoes a gradual cooling process. As the pressure difference becomes larger, the cooling process is faster.

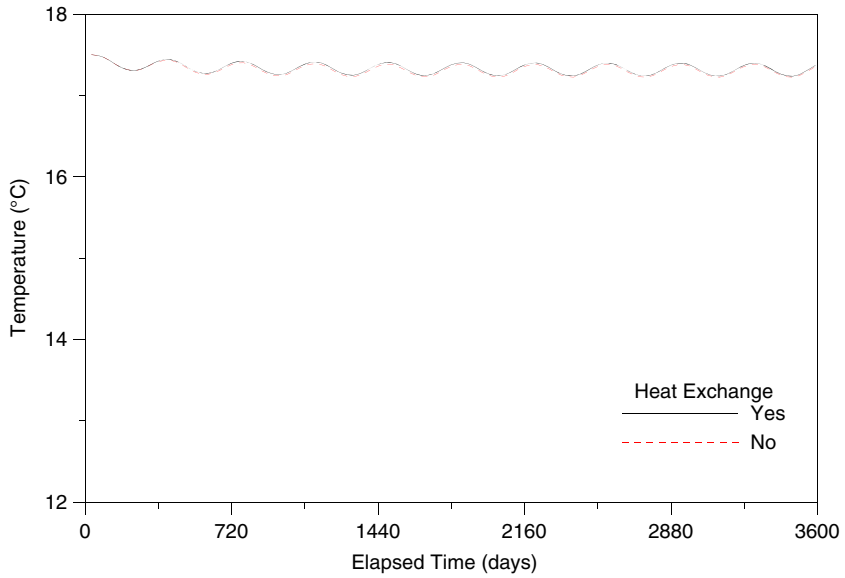

(a)

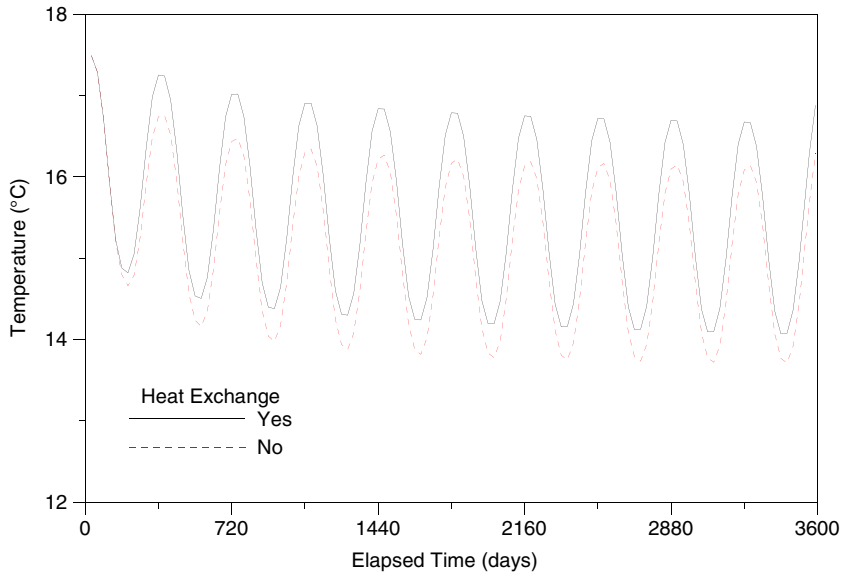

(b)

Fig. 4 Temperature of produced water obtained from simulations with different heat exchange conditions (Δp=40 kPa). Groundwater flow **a** from right to left, **b** from left to right

 DOI 10.1007/s10040-013-1052-6

Reflecting the changes in temperature of the injected water, the temperature of the recovered water fluctuates over a quarter-year period. The temperatures variations at the producing well were constant within the range of 0.94–2.60 °C for the case of left to right groundwater flow and 0.16–0.94 °C for the case of right to left groundwater flow through the 10-year period. Differences in temperature variation among cases are quite significant, more than 2.7 or 5.8 times depending on the pressure difference. The range of variation of Δp=40 kPa is the highest and 16 times higher than that of Δp=−40 kPa, which is the smallest. As the net change of thermal energy is small, the groundwater flow conditions under large pressure gradient and opposite direction to the injected water are more promising.

Heat exchange

Heat transfer from/to overburden and underburden formations is considered as an important factor that controls the temperature of produced water. In the present work, results from the base case were compared with those from a case in which heat exchange is not included. These formations are assumed to have the same aquifer thermal properties as stated earlier.

Figure 4 shows these results at different times with Δp=40 kPa where the largest difference between results is obtained. With groundwater flow from right to left, the inclusion of heat exchange effect makes only a slight difference. Contrarily, the temperature at the production well shows considerable difference under the groundwater

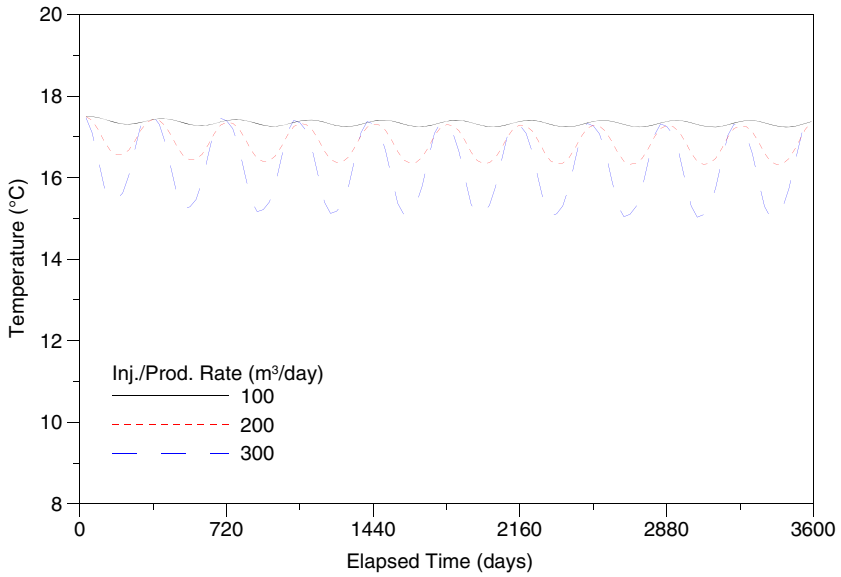

Fig. 5 Temperature of produced water obtained from simulations with different injection/production flow rates (Δp=40 kPa). Groundwater flow **a** from right to left, **b** from left to right

 DOI 10.1007/s10040-013-1052-6

flow from left to right. The temperature remains higher with heat exchange due to the higher temperature of the confining layers compared with the average temperature of the injected water. The results indicate that conductive heat exchange with the surrounding rock may be an important process causing a different cycle of temperature variations in the production well.

Flow rate

The aim of this simulation is to evaluate the recovery of thermal energy from the aquifer given certain injection or production flow rates. The calculations were performed for well and aquifer configurations which are the same as the base case. However, in this simulation, the flow rates are changed to 100, 200, and 300 m^3/day.

The profiles in Fig. 5 show increasing range in temperature of recovered water with increasing flow rate in accordance with the gradual drop over time. By increasing the flow rate from 100 to 300 m^3/day, a significant increase in the variation of temperature is obtained. Tripling the flow rate results in an increase of temperature variation by 13.8 times from 0.16 to 2.22 °C for Δp=−40 kPa and 2.6 times from 2.60 to 6.80 °C for Δp=40 kPa.

The result suggests that, everything else being the same, the use of a lower flow rate, opposite to the direction of regional groundwater flow, is a promising flow condition due to small net change in thermal energy.

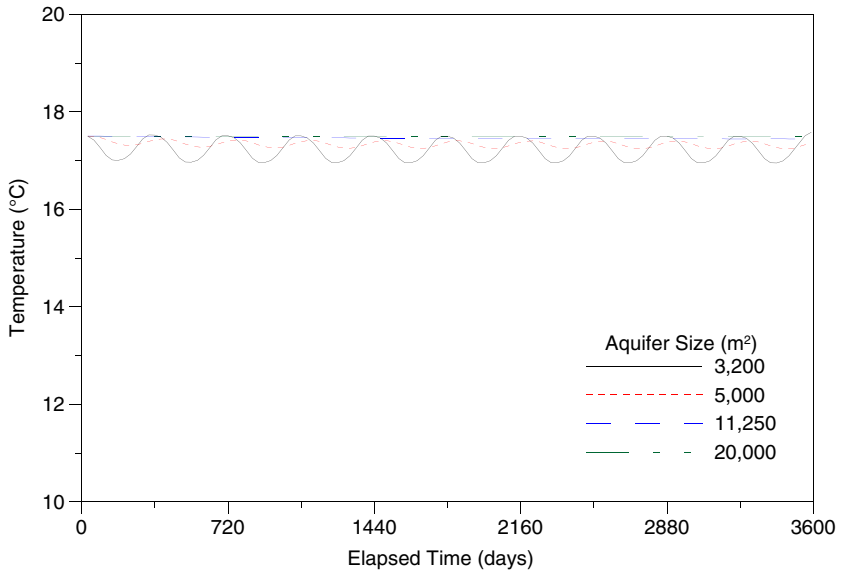

Fig. 6 Temperature of produced water obtained from simulations with different aquifer sizes (Δp=40 kPa). Groundwater flow **a** from right to left, **b** from left to right

 DOI 10.1007/s10040-013-1052-6

However, decreasing the flow rate considerably less than an appropriate value would not be effective because the resulting decrease in the amount of available thermal energy would be a problem.

Aquifer size

One objective with the numerical simulations is to find the well configuration to make the energy storage as dense as possible. In attempts to investigate effects of aquifer drainage size, pumping and injection of groundwater were simulated for four cases considered, 80 m×40 m (3,200 m^2), 100 m×50 m (5,000 m^2), 150 m×75 m (11,250 m^2), and 200 m×100 m (20,000 m^2), in which the aspect ratios of the simulation domain remain 2×1. Accordingly, the injection and production wells are located 40, 50, 75, and 100 m apart, respectively.

Figure 6 illustrates that a larger aquifer size reduced the variations in thermal storage substantially. Larger variations for a small aquifer result from the fact that the thermal front of injected water approaches the production well within each operation period. Therefore, the region near a producing well is considerably affected by injected water. This observation emphasizes the importance of ensuring that adequate spacing between ATES systems is used, taking into account the thermal and hydraulic transport of injected water.

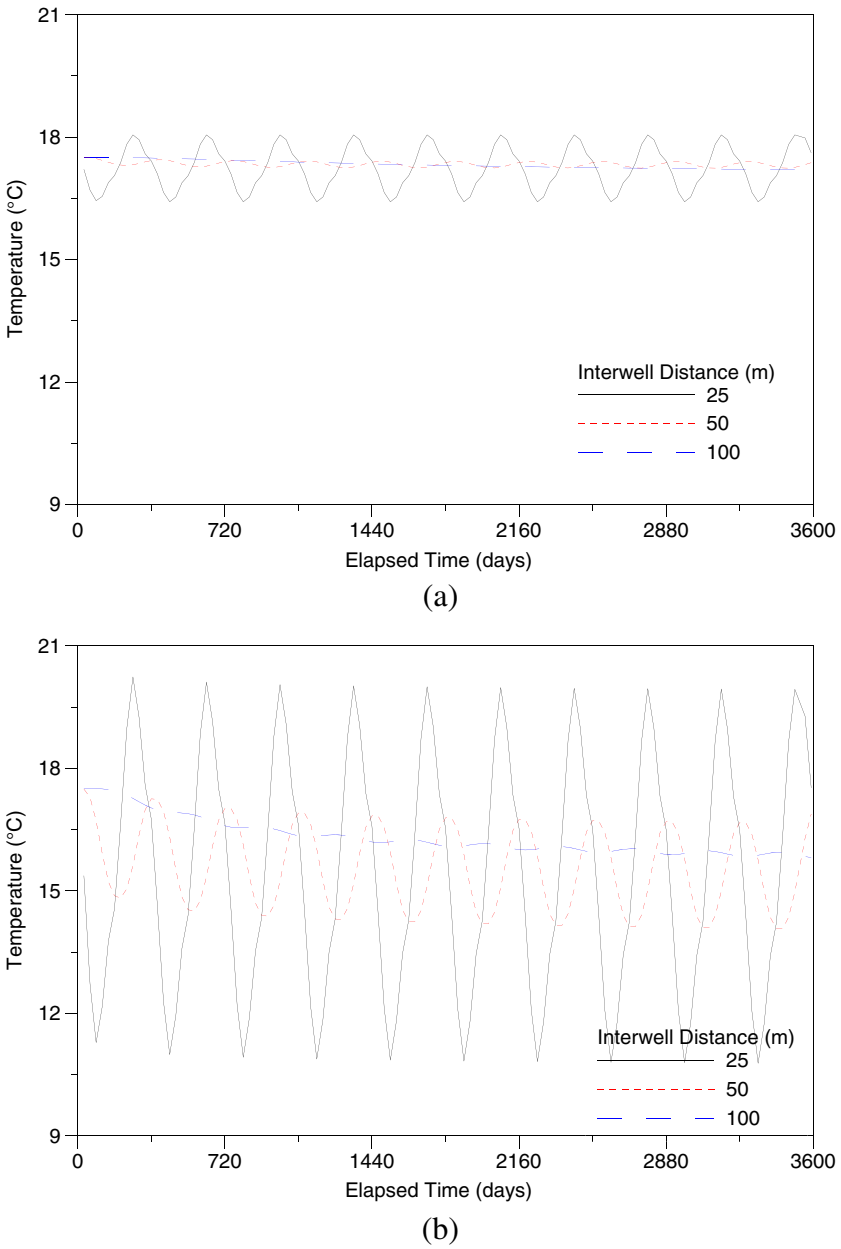

Fig. 7 Temperature of produced water obtained from simulations with different interwell distances (Δp = 40 kPa). Groundwater flow **a** from right to left, **b** from left to right

 DOI 10.1007/s10040-013-1052-6

Interwell spacing

As an attempt to find appropriate well configuration, additional simulations have been performed to examine effects of interwell distance. Pumping and injection of groundwater were simulated for three cases including 50 m×50 m, 100 m×50 m, 200 m×50 m. The length in the x-direction increases while keeping the width in the y-direction the same. The injection and production wells are located at the centers of left and right rectangles consisting of the whole simulation field. Therefore, interwell distances between injection and production wells are 25, 50, and 100 m, respectively.

Figure 7 illustrates how a longer well-to-well distance leads to substantially reduced variations in thermal storage. Temperature variation decreases from 1.64 to 0.31 °C for $\Delta p = -40$ kPa and 9.46 to 1.69 °C for $\Delta p = 40$ kPa as interwell distance increases. Without regional groundwater flow, the temperature variation ranges from 0.96 to 4.71 °C, depending on the interwell spacing. For shorter well-to-well distance, a producing well is considerably affected by injected water and shows quite a significant temperature variation in the produced water. The result emphasizes the need for adequate distance between wells, especially under the situation where regional groundwater flows in the same direction as the injected water.

Conclusions

Numerical calculations were carried out to estimate long-time thermal behavior of an ATES system with two wells under continuous operation. The effects of various geometrical and operational parameters on computed values of aquifer thermal behavior and final producing temperature under regional groundwater flow were studied for a 10-year continuous injection and withdrawal scenario. The hypothetical simulations indicate that the model of the two-well system will be a valuable tool in determining the sensitivity of various parameters.

The performance of the ATES system mainly depends on the thermal interference between stored warm and cold thermal energy in the aquifer. According to the thermo-hydraulic modeling of a continuous mode, the heat transfer in the ATES was affected by a number of factors such as flow conditions of injecting and producing water (temperature and flow rate), groundwater velocity and properties (hydraulic gradient), and aquifer characteristics (heat exchange and size). The thermal behavior of the storage system is shown to depend on the direction and velocity of the groundwater flow, which is determined by regional pressure gradient. Low flow rate opposite to the direction of regional groundwater flow and large aquifer size are recommended as an effective ATES system because of small loss and little fluctuation in extracted thermal energy. When the direction of regional groundwater flow is the same as that of injected water, the thermal front approaches the producing well much closer due to increased thermal convection and results in large variations in the temperature of recovered water. The differences in temperature variation among cases depend on the pressure differences.

Acknowledgements This work was supported by the Energy Efficiency & Resources of the Korea Institute of Energy Technology Evaluation and Planning (KETEP) grant funded by the Korea government Ministry of Trade, Industry and Energy (No. 20122010200060).

References

Allen DM, Ghomshei MM, Sadler-Brown TL, Dakin A, Holtz D (2000) The current status of geothermal exploration and development in Canada. Proc World Geotherm Congr, Kyushu-Tohoku, Japan, May 2000, pp 55–58

Center for Petroleum and Geosystems Engineering (2000) UTCHEM-9.0: a three-dimensional chemical flood simulator. Univ. of Texas at Austin, Austin, TX

Chavalier S, Banton B (1999) Modelling of heat transfer with the random walk method, part 1: application to thermal storage in porous aquifers. J Hydrol 222(1–4):129–139

Doughty C, Hellström G, Tsang CF, Claesson J (1982) A dimensionless parameter approach to the thermal behavior of an aquifer thermal energy storage system. Water Resour Res 18(3):571–587

Fan R, Jiang Y, Yao Y, Shiming D, Ma Z (2007) A study on the performance of geothermal heat exchanger under coupled heat conduction and groundwater advection. Energy 32(11):2199–2209

Kim J, Lee Y, Yoon WS, Jeon JS, Koo M-H, Keehm Y (2010) Numerical modeling of aquifer thermal energy storage system. Energy 35(12):4955–4965

Lee KS, Jeong SJ (2008) Numerical modeling on the performance of aquifer thermal energy storage system under cyclic flow regime. Int J Green Energy 5(1–2):1–14

Liu J, Delshad M, Pope GA, Sepehrnoori K (1994) Application of higher order flux-limited methods in compositional simulations. J Transp Porous Media 16(1):1–29

Molson JW, Frind EO, Palmer CD (1992) Thermal energy storage in an unconfined aquifer, 2: model development, validation, and application. Water Resour Res 28(10):2857–2867

Molz FJ, Warman JC, Jones TE (1978) Aquifer storage of heated water: part I, a field experiment. Ground Water 16(4):234–241

Molz FJ, Parr AD, Andersen PF, Lucido VD, Warman JC (1979) Thermal energy storage in a confined aquifer: experimental results. Water Resour Res 15(6):1509–1514

Molz FJ, Parr AD, Andersen PF (1981) Thermal energy storage in a confined aquifer: second cycle. Water Resour Res 17(3):641–645

Nagano K, Mochida T, Ochifuji K (2002) Influence of natural convection on forced horizontal flow in saturated porous media for aquifer thermal energy storage. Appl Therm Eng 22(12):1299–1311

Nassar Y, ElNoaman A, Abutaima A, Yousif S, Salem A (2006) Evaluation of the underground soil thermal storage properties in Libya. Renew Energy 31(5):593–598

Paksoy HO, Andersson O, Abaci H, Evliya H, Turgut B (2000) Heating and cooling of a hospital using solar energy coupled with seasonal thermal energy storage in aquifer. Renew Energy 19(1–2):117–122

Paksoy HO, Gurbuz Z, Turgut B, Dikici D, Evliya H (2004) Aquifer thermal storage (ATES) for air-conditioning of supermarket in Turkey. Renew Energy 29(12):1991–1996

Papadopulos SS, Larson SP (1978) Aquifer storage of heated water. 2. Numerical simulation of field results. Ground Water 16(4):242–248

 DOI 10.1007/s10040-013-1052-6

Probert T, Hellsröm G, Glaesson J (1994) Thermohydraulic evaluation of two ATES projects in southern Sweden. Proc Int Symp Aquifer Therm Energy Storage, Tuscaloosa, AB, USA, November 1994, pp 73–81

Rafferty K (2003) Ground water issues in geothermal heat pump systems. Ground Water 41(4):408–410

Rosen MA (1999) Second-law analysis of aquifer thermal energy storage systems. Energy 24(2):167–182

Sanner B (2001) Shallow geothermal energy. GHC Bull 22(2):19–25

Schmidt T, Mangold D, Muller-Steinhagen H (2003) Seasonal thermal energy storage in Germany. Proc ISES Solar World Congr, Gothenburg, Sweden, June 2003, pp 1–7

Tenma N, Yasukawa K, Zyvoloski G (2003) Model study of thermal storage system by FEHM code. Geothermics 32(4–6):603–607

Tsang CF, Buscheck T, Doughty C (1981) Aquifer thermal energy storage: a numerical simulation of Auburn University field experiments. Water Resour Res 17(3):647–658

 DOI 10.1007/s10040-013-1052-6